Simplified analytical model for tapered sandwich beams using variable stiffness materials

Qing Ai and Paul M.Weaver

Abstract

A simplified layer-wise sandwich beam model to capture the effects of axial stiffness variation from a combination of geometric taper and variable stiffness properties of the core on the static response of sandwich beam is developed. In the present model, the face sheets are assumed to behave as Euler beams and the core is modelled with a first order shear deformation theory. With geometrical compatibility enforced at both upper and lower skin/core interfaces, the beam's field functions are reduced to only three, namely the extensional, transverse and rotational displacements at the mid-plane of the core. The minimum total potential energy method is used in combination with the Ritz technique to obtain an approximate solution. Geometrically nonlinear effects are considered in the present formulation by introducing *von Kármán* strains into the face sheets and core. Two types of sandwich beams, uniform and tapered, with different boundary conditions are studied. Results show that the proposed model provides accurate prediction of displacements and stresses, compared to three dimensional finite element analysis. It is found that due to the axial stiffness variation in the core, displacements of beams and stresses of face sheets and core are significantly affected. The potential design space is shown to be expanded by utilizing variable stiffness materials in sandwich constructions.

Keywords

variable stiffness, sandwich beams, axially graded core, Ritz method, non-linear model

Introduction

Composite materials and their structures have received growing interest in recent decades from industry and researchers for their excellent performance. Of particular interest are laminated sandwich structures for their wide ranging applications in the aerospace, automobile and marine industries due to superior structural properties combined with light weight. Furthermore, as material costs of carbon- and glass- fibre composites, and metallic and nonmetallic foam/cores reduce, the potential of sandwich constructions increases [1].

Various analysis tools including finite element method (FEM)[2, 3] and analytical models [4–7], have been developed for composite structures including sandwich beams, for efficient and accurate structural analysis purposes. FEM is able to provide a wider versatility and modelling flexibility than analytical models, while requiring high computational expense. However, analytical models offer the physical insight of the problem and can be widely used for the preliminary design. Extensive literature concerning analytical models of static and dynamic response for sandwich beams is available in Ref. [4–13]. In sandwich beam models, skins are usually modelled using beam models including Euler and Timoshenko beam theories and one main difference among them is the way in which the honeycomb core is considered. Among available sandwich beam models, the transverse compressibility of the core is either ignored [4, 5] or modelled using elasticity theory [6, 7]. Rao [4] developed an analytical approach to investigate the effect of extensional and bending stiffness in a stiff core on the overall static response of sandwich beams. Assuming that the face sheets act as Euler beams and the transversely incompressible honeycomb core behaves as a Timoshenko beam, the governing equations were derived using three field variables:

- transverse deflection of the beam,

Advanced Composites Centre of Innovation and Science, Department of aerospace engineering, University of Bristol

Corresponding author:
Qing Ai, Advanced Composites Centre of Innovation and Science, University of Bristol, Queen's Building, University Walk, Bristol, BS8 1TR, UK
Email: qing.ai@bristol.ac.uk

- extension of the top skin's mid-plane,
- extension of the bottom skin's mid-plane.

With a variational method, the governing differential equations were solved via Laplace transforms. Results showed that the effect of core stiffness on beam deflection and stresses can be significantly high for stiff-cored, thick-cored or highly unsymmetric sandwich beams. Jeon [5] presented a new formulation to analyse the bending behaviour of tapered sandwich plates constituting an orthotropic core of unidirectional linear thickness variation and two uniform anisotropic composite skins. The minimum total potential energy method was used to derive the governing equations and approximate solutions were obtained with the Ritz method. With geometric coupling between the core transverse shear strain and the face normal deflection considered, effects of edge conditions, taper ratios, core moduli ratios and stacking sequence of the laminated skins on the structural deflection were parametrically studied. In the sandwich beam model developed by Frostig [6, 7], namely the higher-order sandwich panel theory (HSAPT), skins are modelled with Euler beam theory and the transversely flexible core is modelled with a two-dimensional elasticity theory. The bending behaviour of the sandwich beam was studied in terms of internal stress resultants and displacements in skins, peeling and shear stresses in skin-core interfaces and stresses and displacement fields of the core. Moreover, the nonlinear displacement fields through the depth of the core were also determined.

Recent material technology advent has introduced novel skin and core/foam materials into sandwich constructions. In addition to conventional metallic, polymeric foam and core, functionally graded materials (FGM) have been used in sandwich plates [14–17]. FGM refers to materials of which mechanical properties vary continuously and mostly through the thickness of a structure [16, 17]. Static and dynamic response of FGM beams have received increasing attention recently [18–21] due to their potential for optimizing structural weight and mechanical properties. Zenkour [14, 15] systematically investigated the static and dynamic behaviours of simply supported transversely FGM ceramic-metal sandwich beams. Deflection and stresses of a three-layer sandwich plate of uniform thickness were predicted using a sinusoidal shear deformation plate theory. It was found that the mechanical response of the sandwich beam was highly dependent on the FGM properties. Tounsi [16] presented a refined shear deformation theory to predict the thermoelastic bending behaviour of FGM sandwich plates. The material volume fraction was assumed to obey a power law function through the thickness of the beam and then the Young's modulus and thermal expansion coefficient were calculated via the

rule of mixtures. The proposed model provided accurate results against other methods reported in the literature.

The current work presents an extension of Rao's [4] three-layer sandwich beam theory, which further considers sandwich beams of tapered geometry and honeycomb cores of variable axial stiffness. Using the present formulations, the static response of sandwich beams with cores of variable axial stiffness has been studied and different beam geometries and boundary conditions are studied. In the following sections, formulations are presented in detail and results are then discussed in order to qualitatively assess the effect of axial stiffness variation in the core on the static response of sandwich beams.

Mechanics of the layer-wise sandwich beam model

A sandwich beam with length (L), width (b), and core, upper and lower skins thickness of ($2h_c$), ($2h_u$) and ($2h_l$) respectively, is shown in Figure 1, with three local coordinate systems defined for each layer. Key assumptions are:

(1). face sheets are made of linear elastic materials and satisfy Euler beam theory;
(2). the honeycomb core resists through-thickness deformation and is formulated using a first order shear deformation theory;
(3). face sheets are perfectly bonded to the core with negligible adhesive layer thickness.

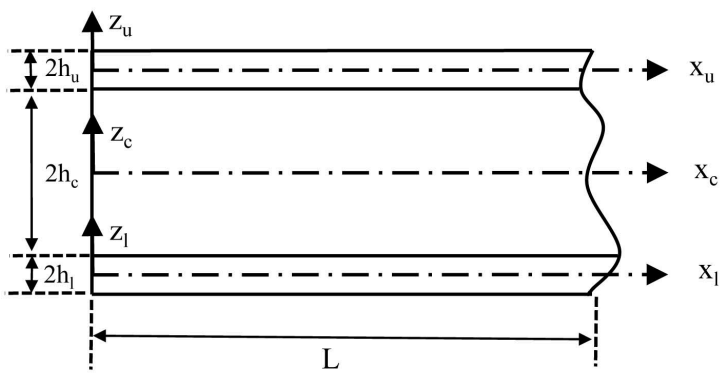

Figure 1. Sandwich beam geometry and co-ordinates

Displacement fields and strains

As shown in Figure 1, displacement fields in all three layers of the sandwich beam are described using the local coordinate systems:

$$\begin{aligned} u_{x\xi} &= u_\xi(x_\xi) - z_\xi \varphi_\xi(x_\xi); \\ u_{y\xi} &= 0; \\ u_{z\xi} &= w_\xi(x_\xi) \end{aligned} \tag{1}$$

where, $\xi = u, c, l$ refer to the upper skin, core and lower skin respectively. With the aforementioned assumptions, both the upper and lower skins are modelled as Euler beams, which leads to the reduction of relevant field variables:

$$\begin{aligned} \varphi_u(x_u) &= w_u^{'}(x_u) \\ \varphi_c(x_c) &= \varphi(x) \\ \varphi_l(x_l) &= w_l^{'}(x_l) \end{aligned} \tag{2}$$

Now, the beam is governed by seven state displacement functions: extensional and transverse displacements at the centroids of top and bottom skins and extensional, transverse and rotational deformation at the mid-plane of the honeycomb core. With the enforced geometry compatibility conditions at the upper and lower face/core interfaces applied:

$$\begin{aligned} w_c(x) &= w_u(x) \\ u_c(x, h_c) &= u_u(x) + h_u w_u^{'}(x) \\ w_c(x) &= w_l(x_l) \\ u_c(x, -h_c) &= u_l(x) - h_l w_l^{'}(x) \end{aligned} \tag{3}$$

the extensional and transverse displacement at the mid-plane of face sheets are explicitly expressed in terms of core field functions:

$$w_u(x) = w_c(x), \tag{4a}$$

$$u_u(x, z_u) = u_c(x) - h_c \varphi(x) - (h_u + z_u) w_c^{'}(x), \tag{4b}$$

$$w_l(x) = w_c(x_c), \tag{4c}$$

$$u_l(x, z_l) = u_c(x) + h_c \varphi(x) + (h_l - z_l) w_c^{'}(x), \tag{4d}$$

With the algebraic equations in Equation. 4 , the state functions of the sandwich beam is further reduced to only three: the transverse, extensional and rotational displacements at the mid-plane of the honeycomb core, $\{w_c, u_c, \varphi_c\}$. The strain-displacement relations of face sheets and core are [22]:

$$\begin{aligned} &\varepsilon_{xx,\xi} = \varepsilon^0_{xx,\xi} + z_\xi \varepsilon^1_{xx,\xi}, \\ &\gamma_{xz,\xi} = \gamma^0_{xz,\xi}, \\ &\varepsilon^0_{xx,\xi} = \frac{du_\xi}{dx_\xi};\ \varepsilon^1_{xx,\xi} = \frac{d\varphi_\xi}{dx_\xi};\ \gamma^0_{xz,\xi} = \frac{dw_\xi}{dx_\xi} - \varphi_\xi, \end{aligned} \tag{5}$$

where, $\xi = u, c, l$. The strain components can be derived algebraically using the aforementioned three state functions and therefore the total potential energy of the beam can be also calculated using the same functions.

The Ritz method

Combined with the Ritz method, the minimum total potential energy principle is applied to obtain an approximate solution of the present formulation. The total energy of the deflected sandwich beam constitutes the strain energy (U) of face sheets (Π_u, Π_l) and core (Π_c), and the potential of the external loads (V), are:

$$\delta(U + V) = 0, \tag{6a}$$

$$U = \Pi_u + \Pi_l + \Pi_c, \tag{6b}$$

$$V = \Pi_e, \tag{6c}$$

For laminated composite face sheets considered in this model, the layup is assumed to be symmetric and balanced and classical laminate analysis is applied to calculate the skin's equivalent stiffness [23]. Assumption is made here that there is no variation in displacements, strains and stresses in the beam width direction. The strain energy of the face sheets in Eq.6b is derived in terms of strain components from Eq.5:

$$\begin{aligned} \Pi_u &= 0.5 \oint_{V_u} (\sigma_{xx,u} \cdot \varepsilon_{xx,u}) dv_u \\ &= 0.5 \int_{x_u} \int_{y_u} \int_{z_u} (\sigma_{xx,u} \cdot \varepsilon_{xx,u}) dx_u dy_u dz_u \\ &= 0.5 \int_{x_u} \int_{y_u} \int_{z_u} (Q^*_{11,u} \cdot (\varepsilon_{xx,u})^2) dx_u dy_u dz_u \\ &= 0.5b \int_{x_u} \{A_{11,u} \cdot (\varepsilon^0_{xx,u})^2 + D_{11,u} \cdot (\kappa_{xx,u})^2\} dx_u \end{aligned} \tag{7}$$

where, A_{11} and D_{11} are components of the extensional and bending stiffness matrices of the laminated skin [23], $Q^*_{11,u}$ is an element in the transformed reduced stiffness matrix of the ply and κ_{xx} is the midplane curvature of the deflected skin. However, the strain energy of the core comprises extensional, bending and transverse shear deformation [4]:

$$\begin{aligned}\Pi_c &= \frac{1}{2}\int_0^L (E_c(x)\cdot A_c(x)\cdot (u_c^{'}(x))^2 \\ &+E_c(x)\cdot I_c(x)\cdot(\varphi_c^{'}(x))^2 + G_c(x)\cdot A_c(x)\cdot(w_c^{'}(x)-\varphi_c(x))^2)dx\end{aligned} \tag{8}$$

where, A_c is the cross-section area of the core and I_c refers to the second moment of area relative to its local x axis.

The external work by the external forces is:

$$\begin{aligned}\Pi_e &= -\int_0^L (n_x u_c(x) + q_x w_c(x) + m_x \varphi_c(x))dx + \\ &\int_0^L (N_x u_c(x) + P_x w_c(x) + M_x \varphi_c(x))\delta(x-x_k)dx\end{aligned} \tag{9}$$

where, n_x, q_x and m_x are the distributed in-plane, transverse external forces and bending moment; N_x, P_x and M_x are concentrated in-plane, transverse forces and bending moment and $\delta(x-x_k)$ is the Dirac delta function at the positions where external loads are applied.

In the Ritz method, the displacement functions are expanded in series of admissible functions satisfying the essential boundary conditions. The displacement field of the honeycomb core are assumed to be:

$$\begin{aligned}w_c(x) &= \sum_{i=1}^{N} a_i w_i(x) \\ u_c(x) &= \sum_{i=1}^{N} b_i u_i(x) \\ \varphi_c(x) &= \sum_{i=1}^{N} c_i \varphi_i(x)\end{aligned} \tag{10}$$

where $w_i(x), u_i(x), \varphi_i(x)$ are the admissible functions of the transverse, extensional and rotational displacements and N refers to the order of expansions. By combining Eqs. 1 to 10 and making appropriate reductions leads to the following linear system of expressions:

$$\begin{bmatrix}[A] & [B] & [C] \\ [D] & [E] & [F] \\ [G] & [H] & [K]\end{bmatrix}\begin{Bmatrix}\{a\} \\ \{b\} \\ \{c\}\end{Bmatrix} = \begin{Bmatrix}\{F_1\} \\ \{F_2\} \\ \{F_3\}\end{Bmatrix} \tag{11}$$

Elements of the stiffness matrices and modal force matrix are given in Appendix A.

The nonlinear formulations

For beams under large deflection, geometric nonlinearity plays a significant role in static response [12, 24]. The nonlinear kinematic relations of the face sheets and core are based on *von Kármán* strains [24] and the only non-zero strains are:

$$\begin{aligned} &\varepsilon_{xx,\xi} = \varepsilon^0_{xx,\xi} + z\varepsilon^1_{xx,\xi}, \\ &\gamma_{xz,\xi} = \gamma^0_{xz,\xi}, \\ &\varepsilon^0_{xx,\xi} = \frac{du_\xi}{dx_\xi} + \frac{1}{2}(\frac{dw_\xi}{dx_\xi})^2;\ \varepsilon^1_{xx,,\xi} = \frac{d\varphi_\xi}{dx_\xi};\ \gamma^0_{xz,\xi} = \frac{dw_\xi}{dx_\xi} - \varphi_\xi, \end{aligned} \tag{12}$$

where $\xi = u, c, l$. The resulting Rayleigh-Ritz expression, in comparison with Eq.11 becomes nonlinear and are solved with iterative methods [12, 24], such as the Newton-Raphson technique.

Using the Ritz method, the minimum total potential energy principle can be re-written in the following matrix form [24]:

$$[K(q_i)]\, q_i - [F_i] = 0 \; or \; [R(q_i)] = 0 \tag{13}$$

where $[K]$ is the nonlinear stiffness matrix, which depends on the undetermined coefficients q_i; $[F]$ is the generalized force vector; $[R]$ represents the residual vector or unbalanced force vector [24].

In the Newton-Raphson method, the formulations is solved by iteratively evolving q_i which reduces the unbalanced force vector to an acceptably small residual value, $\varepsilon_{criteria}$. The solution at the $(n+1)th$ iteration is obtained using the nth iteration solution and the tangent matrix, $[T]$,

$$\{q_i\}_{n+1} = \{q_i\}_n - [T(q_i)_n]^{-1}[R(q_i)_n] \tag{14}$$

At the beginning of the iteration, an initial solution needs to be provided, which can be arbitrary and the solution is updated at each iteration until the unbalanced force vector approaches the termination criteria, $|R(q_i)| < \varepsilon_{criteria}$. Elements of matrix $[T]$ and $[R]$ are defined in Appendix B.

Numerical results and discussions

In this section, the static response of uniform thickness and tapered sandwich beams are investigated using the proposed model. Both the linear model (LM) and nonlinear model (NLM) are used in the following sections and results are compared against that from three dimensional finite element methods (FEM, ABAQUS). Comparison studies are also performed in order to validate the accuracy of present model. Convergence studies have been performed and a significant finding is that a series expansion order of 10-12 appears to provide a reasonable balance between results accuracy and computational expense. Note, higher order polynomials are prone to ill-conditioning and numerical instabilities, which leads to loss in results accuracy [25, 26].

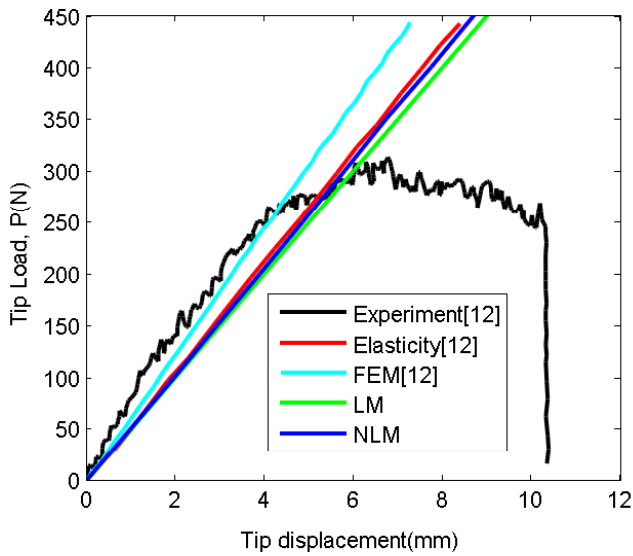

Figure 2. Comparison of the present model with the literature [27]

Comparison studies

Firstly, the results of present model are compared with that of a finite difference method (FDM) and experimental tests in Ref.[9] and an analytical approach from Ref.[5]. The face sheets of the sandwich beam are Al alloy of Young's modulus 68.17 GPa and the shear moduli of the core is 3.68 MPa. The beam is simply supported at both ends with its thickness linearly decreasing from middle towards the ends. A distributed load, P,

Table 1. Quasi-stiffness ($P/(\delta_1 - \delta_2)$, kPa) of a tapered sandwich beam

H_r	FDM [9]	Exp [9]	Analytical model [5]	Present
1.00	1772	1772	1773.8	1772.2
1.11	1848	1779	1851.3	1847.5
1.43	2034	1986	2047.5	2035.3
2.00	2289	2282	2332.5	2295.7

Table 2. Material properties of the sandwich beam [27]

Materials	Properties
AS4/3501-6 Carbon/epoxy prepreg layup of $[0/90]_s$	Equivalent homogeneous E=68300 MPa, ν = 0.05
Polyurethane foam	E=31.6 MPa, G= 11.22 MPa, ρ= 96 kg/m^3

is applied at the mid-span of the span along the beam width and displacements of two selected span-wise positions, 10.2 mm and 44.2 mm from one end, are recorded as δ_1 and δ_2 respectively. The taper ratio, H_r, i.e. the ratio of the root to tip thickness of core, is used to define the thickness variation. The *quasi stiffness* is calculated using external load and deflections, $P/(\delta_1 - \delta_2)$, and results from the present model and literature are shown in Table.1. The present model gives results in good correlation with experimental data and has about 0.7% less error compared with the FDM and analytical model from Ref.[5].

]A sandwich beam of uniform thickness is also investigated using the present method. The specimen size is: laminated face sheets thickness= 0.526 mm, core height= 6.35 mm, span length= 152.4 mm and beam width= 25.4 mm. Material properties are shown in Table.2. The beam is simply supported at its ends and subject to distributed load along the beam width at the mid-span where the beam deflection is measured. The present model is compared with experiment and elasticity theory [27] and good agreement is found, as shown in Figure 2. However, the discrepancy between experiments, elasticity theory and the present linear model, is caused by an increased stiffness of the thick adhesive layer due to the penetration of adhesive in to the high porosity regions of the core [27].

Table 3. Mechanical properties of core used in C-C sandwich beams

Material	Case	E (MPa) and ν (-)
Carbon/epoxy, [90/0/90]	-	E=56900, $\nu = 0.05$
Core	A	PVC foam, $E(x) = 104$, $\nu = 0.3$ [28]
	B	$E(x) = 104 + 0.92x - 0.0046x^2$, $\nu = 0.3$
	C	$E(x) = 104 - 0.68x + 0.0034x^2$, $\nu = 0.3$

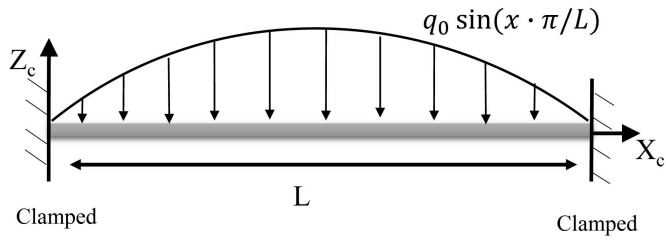

Figure 3. Clamped-clamped sandwich beam subject to sinusoidal distributed load

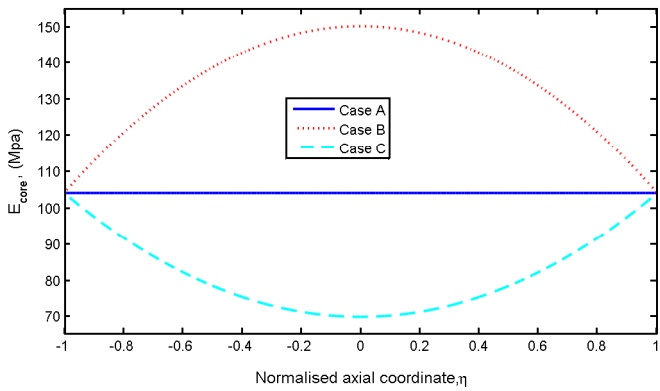

Figure 4. Axial stiffness distribution of Case A, B and C

Uniform thickness sandwich beam with clamped-clamped boundary conditions

In this section, uniform thickness sandwich beams with both ends clamped (C-C) are studied using the present formulation. A beam configuration of length $L = 200$ mm, width $b = 20$ mm, face sheets thickness $2h_{u,l} = 0.4$ mm and core height $2h_c = 14.2$

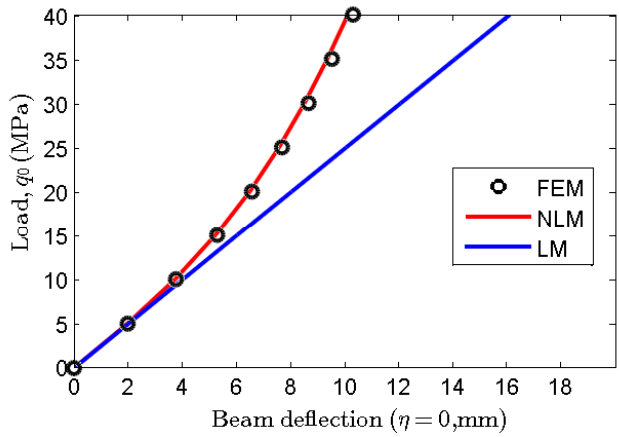

Figure 5. Load-displacement diagram of Beam A

mm is chosen and associated material properties are shown in Table 3. Functionally graded foams with three types of polynomial axial stiffness variation are considered (see Figure 4) while the Poisson's ratio is assumed to remain constant. As shown in Figure 3, a sinusoidal distributed load is applied to the beam, $q(x) = q_0 sin(x \cdot \pi/L)$.

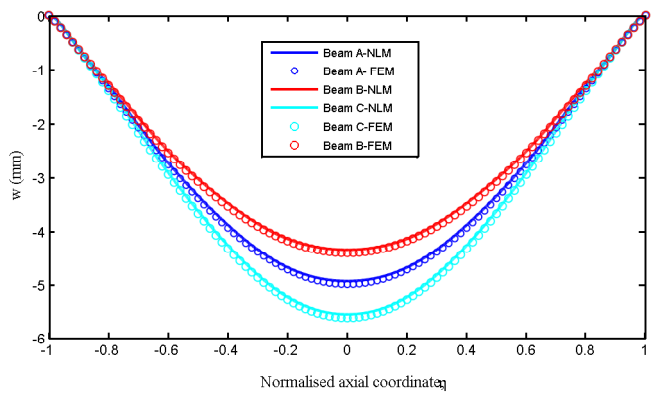

Figure 6. Transverse displacement at the mid-plane of the core of Beam A, B and C

The admissible functions of displacement field are expanded using Legendre polynomials in terms of normalised coordinate $\eta = 2x/L - 1, (\eta \in [-1, 1])$, with C-C type boundary condition applied, as:

$$
\begin{aligned}
w_i(\eta) &= (\eta+1)^2 \cdot (\eta-1)^2 \cdot L_i(\eta) \\
u_i(\eta) &= (\eta+1) \cdot (\eta-1) \cdot L_i(\eta) \\
\varphi_i(\eta) &= (\eta+1) \cdot (\eta-1) \cdot L_i(\eta)
\end{aligned} \tag{15}
$$

and $L_i(\eta)$ are the Legendre polynomials defined as [29],

$$
\begin{aligned}
L_0 = 1, L_1 = \eta, L_2 = \frac{1}{2}(3\eta^2 - 1) \cdots \\
L_i(\eta) = \sum_{j=1}^{J} (-1)^j \frac{(2i-2j)!}{2^i j!(i-j)!(i-2j)!} x^{i-2j}
\end{aligned} \tag{16}
$$

where,

$$
J = \begin{cases} {}^{i}/_{2}, & \textit{(i=0,2,4,6,...)} \\ {}^{(i-1)}/_{2}, & \textit{(i=1,3,4,7,...)} \end{cases}.
$$

At first, the results of the present formulation, both nonlinear (NLM) and linear models (LM) are compared against three dimensional FEM. For Beams A, B and C considered in this section, 8-node C3D8R solid elements were used and after a mesh convergence analysis, 200 elements along the beam length, 10 elements along the beam width and 20 elements through the thickness of skins and core were chosen to discretize the beam. Clamped boundary condition was enforced at both ends and the pressure loads were applied on the top surface. As shown in the load-deflection diagram of Beam A in Figure 5, the nonlinear model provides more accurate beam deflection prediction than the linear model and is subsequently used in this section.

Figure 6 presents the transverse displacement of sandwich beams A, B and C under a sinusoidal load with $q_0 = 14$ Mpa/mm using the present nonlinear model. Results are plotted against that from FEM and is shown to compare well with a maximum 2% error. However, although the core stiffness is much lower than that of the skin ($E_{skin}/E_{core} \approx 500$), a significant change in beam deflection across the three beams is shown in Figure 6. As expected, the in-plane stiffness variation of the core considerably affects the beam's transverse displacement and a stiffer core in Beam B leads to reduction in maximum displacement, which results from an increased effective bending stiffness of the beam and a higher transverse shear modulus in the core. An opposite trend is found in Beam C which has less stiff core than Beams A and B.

The axial stress distribution through the beam thickness at two span-wise position,$\eta = -0.5$ and 0, are shown in Figure 7 and are in good agreement with FEM. It is shown that the axial stress in both top and bottom skins has changed due to the core's stiffness

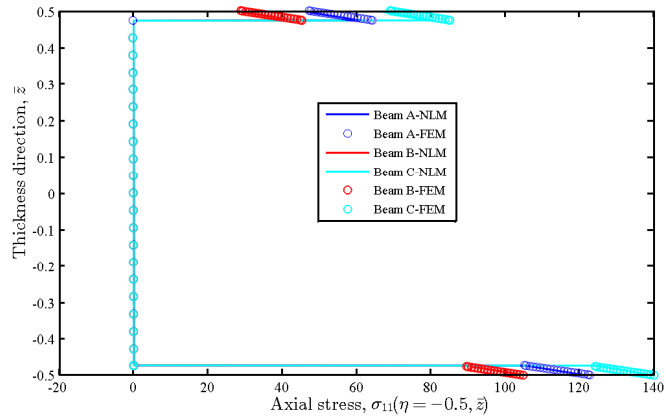

(a) Normal stresses along thickness, $\sigma_{11}(\eta = -0.5, \bar{z})$ (MPa)

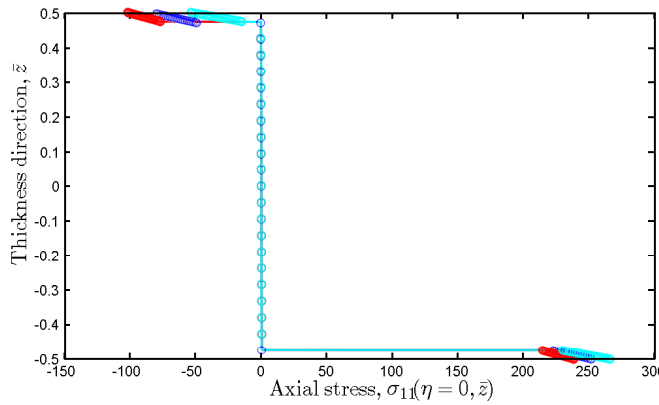

(b) Normal stresses along thickness, $\sigma_{11}(\eta = 0, \bar{z})$ (MPa)

Figure 7. Axial stress distribution along thickness in Beam A, B and C

variation. As shown in Figure 7(a), Beam B has lower axial stresses in the top skin with higher stiffness of core while Beam C presents higher top skin axial stress with lower core stiffness compared to Beam A. The reason is that for indeterminate structures such as beams with C-C boundary conditions, the stress distribution is deformation dependent and therefore, the core's property variation plays an important role in both deflection and stress distribution. Figure 8 shows the linear and nonlinear components of the axial stress, which correspond to the linear and nonlinear component of the strain in Eq 12

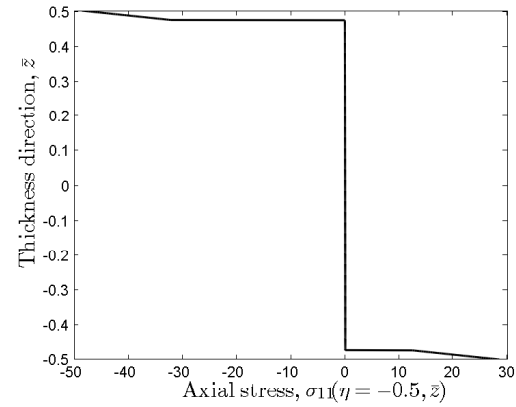

(a) Linear component (MPa)

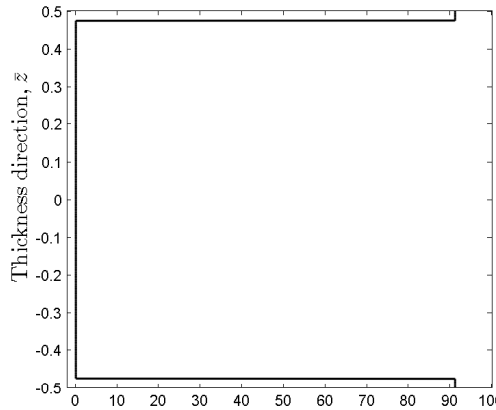

(b) Nonlinear component (MPa)

Figure 8. Through-thickness distribution of linear and nonlinear components of axial stress of Beam A ($\eta = -0.5$)

respectively, through the thickness of Beam A at $\eta = -0.5$, (see Figure 7(a)) and it is found that the linear axial stress satisfies the typical sandwich beam behaviour while the nonlinear membrane stress, see Eq. 12, dominate bending stress in the total axial stress contribution. Furthermore, the transverse shear stress and strain at the mid-plane of the core are also altered, as shown in Figure 9, and the transverse shear strain is affected to a higher level as the transverse shear modulus changes accordingly with the in-plane stiffness.

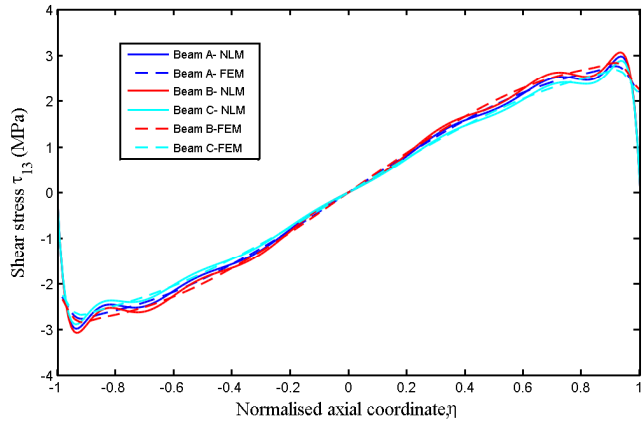

(a) Transverse shear stresses at the mid-plane of the core , τ_{13} (MPa)

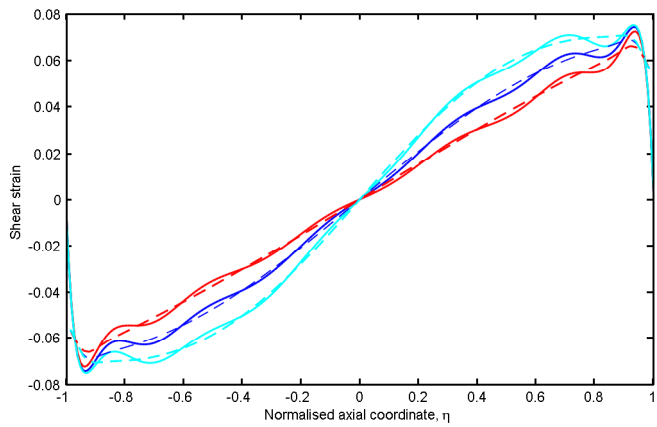

(b) Transverse shear strain at the mid-plane of the core , γ_{13}

Figure 9. Transverse shear stress and strain at the mid-plane of the core for Beam A, B and C

Tapered sandwich beam with clamped-free boundary conditions

Sandwich plates often have non-uniform cross-sections when used in structural components like aircraft wings and control surfaces. In this section, the present formulation is used to investigate the static response of tapered cantilever sandwich beams (C-F boundary condition). The beams are of length, $L = 100$ mm, width $b = 20$ mm, face sheets thickness $2h_{u,l} = 0.4$ mm and core root height $2h_{c,root} = 24.2$ mm with a taper angle $\beta = 5°$, which is the angle between axial axis of face sheets and core.

A transverse tip load, P_0 is applied at the free end. Three different honeycomb core in-plane stiffness distribution are considered, Beams D, E and F as shown in Table 4 (see Figure 10). Figure 11 shows the deflection diagram of Beam D under tip load P where for C-F type beams, both LM and NLM provide accurate results, compared to FEM (ABAQUS, C3D8R elements, 100 elements along beam length, 10 elements along the beam width and 20 elements along the thickness of skins and core), for the load-deflection case considered. LM is used to calculate beam responses in this section and results are compared with that from FEM.

Table 4. Mechanical properties of core used in tapered sandwich beams

Material	Case	E (MPa) and ν (-)
Carbon/epoxy, [0/90/0]	-	E=109000, $\nu = 0.05$
Core	D	PVC foam, $E(x) = 104$, $\nu = 0.3$ [28]
	E	$E(x) = 104 + 0.3x$, $\nu = 0.3$
	F	$E(x) = 104 - 0.8x + 0.01x^2$, $\nu = 0.3$

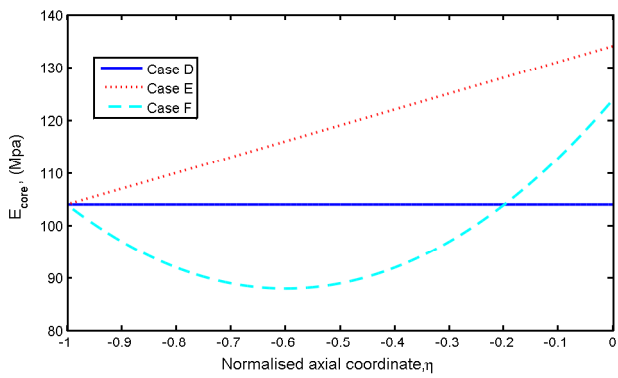

Figure 10. Axial stiffness distribution of Case D, E and F

As shown in Figure 12, the transverse displacements of sandwich beams under tip load $P_0 = -792$ N are affected due to the presence of axial stiffness variation in the core. The tip displacement of Beam E with linearly increased axial core stiffness is reduced by 11% compared to that of Beam D of uniform core stiffness. Furthermore, Beams D and F provide tip displacements that are close in value yet the deformation shape is

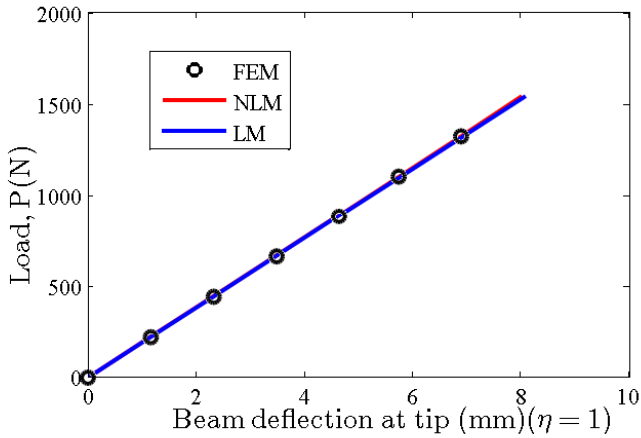

Figure 11. Load-displacement diagram of Beam D

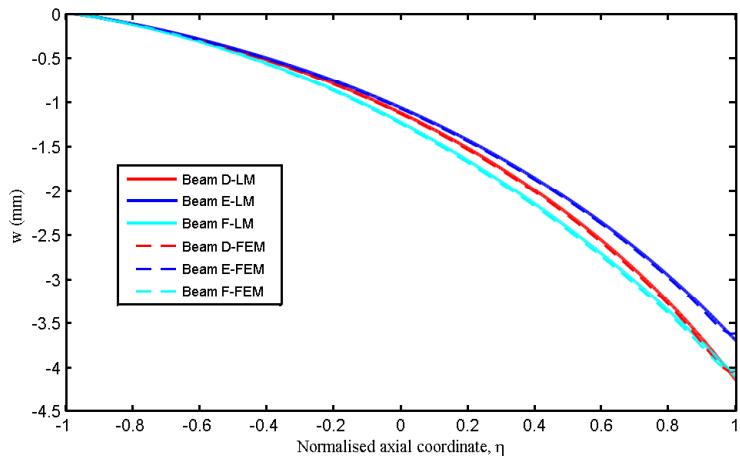

Figure 12. Transverse displacement at the mid-plane of the core of Beam D, E and F

considerably different from each other. Corresponding to the stiffness distribution shown in Figure 10, Beams D, E and F show different slope distributions as a consequence of the change of effective bending stiffness of the cross-section under the same tip load.

The axial stress distribution through beam thickness in Beams D, E and F is shown in Figure 13 and an accuracy within 1% compared to results from FEM is achieved.

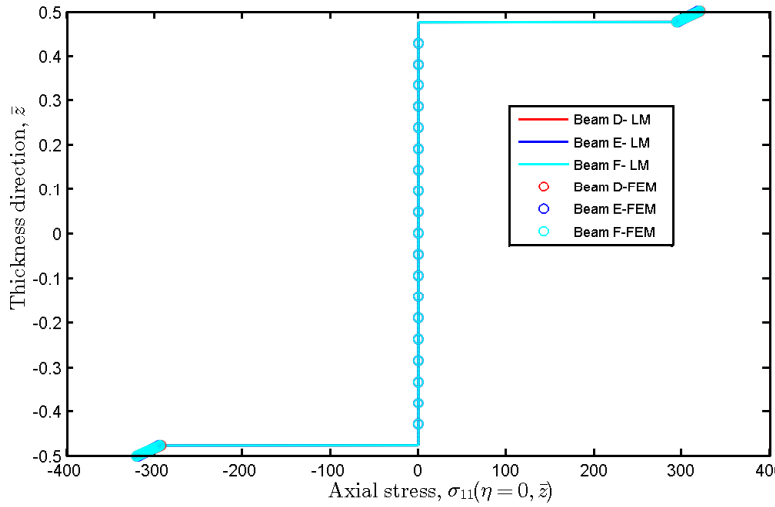

Figure 13. Axial stress distribution through thickness in Beam D, E and F

Similar to the beams of C-C type boundary conditions considered previously, the core's in-plane load-carrying capacity is negligible and most axial load is carried by the top and bottom skins. The effect of core in-plane stiffness variation on axial stress in skins is limited, as shown in Figure 13, which is due to the fact the the variation of the core stiffness is minor compared to skin stiffness. A similar trend is found in the transverse shear stress at the mid-plane of core and no apparent effect of core stiffness variation is noticed (Figure 14(a)). However, the transverse shear strain has been significantly affected because of the variation in the shear modulus and the in-plane Young's modulus, as shown in Figure 14(b).

Conclusions

A novel non-linear layer-wise sandwich beam formulation has been developed by extending Rao's sandwich beam model. Combined with the minimum total energy principle, the Ritz method has been applied to solve both the linear and nonlinear governing equations. Results show that the present model is capable of providing accurate predictions of static response of sandwich beams with different geometries and boundary conditions over a wide range of material properties. Due to the fact that simplifications are made in the beam model and only three field variables are used,

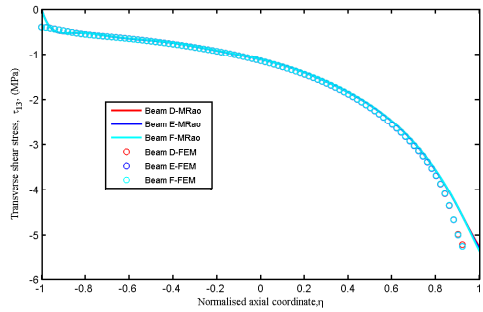

(a) Transverse shear stresses at the mid-plane of the core , τ_{13} (MPa)

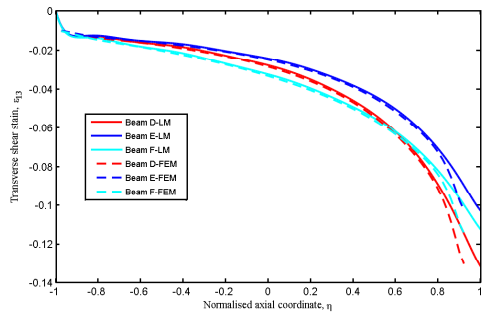

(b) Transverse shear strain at the mid-plane of the core , γ_{13}

Figure 14. Transverse shear stress and strain at the mid-plane of the core for Beam D, E and F

there are indeed some effects that can not be predicted, such as the thickness direction transverse displacement in the core and the transverse shear stress along the beam thickness.

Based on the model, the effects of axial variable stiffness variation of the core on the beam static response have been investigated. It has been found that significant changes in the static response has been achieved via tailoring the core's axial stiffness, which is also dependent on the boundary conditions. For beams with C-C boundary conditions, both stresses and displacements have been affected while for the cantilever beams, stresses are less affected considering the limited variation in core stiffness compared to skin stiffness. With variable stiffness materials utilized, the sandwich beam design space can be considerably extended and the present model can be used as a preliminary design tool for laminated sandwich beams.

Appendix A

The total strain energy of the sandwich beam is :

$$\Pi_{Strain} = \Pi_u + \Pi_l + \Pi_c \tag{17}$$

Elements of stiffness matrix are defined using undetermined coefficients $\{a_i,\ b_i,\ c_i\}$:

$$A_{ij} = \frac{\partial^2 \Pi_{Strain}}{\partial a_i \partial a_j},\ i = 1.....N,\ \ j = 1.....N, \tag{18}$$

$$B_{ij} = \frac{\partial^2 \Pi_{Strain}}{\partial a_i \partial b_j},\ i = 1.....N,\ \ j = 1.....N, \tag{19}$$

$$C_{ij} = \frac{\partial^2 \Pi_{Strain}}{\partial a_i \partial c_j},\ i = 1.....N,\ \ j = 1.....N, \tag{20}$$

$$D_{ij} = \frac{\partial^2 \Pi_{Strain}}{\partial b_i \partial a_j},\ i = 1.....N,\ \ j = 1.....N, \tag{21}$$

$$E_{ij} = \frac{\partial^2 \Pi_{Strain}}{\partial b_i \partial b_j},\ i = 1.....N,\ \ j = 1.....N, \tag{22}$$

$$F_{ij} = \frac{\partial^2 \Pi_{Strain}}{\partial b_i \partial c_j},\ i = 1.....N,\ \ j = 1.....N, \tag{23}$$

$$G_{ij} = \frac{\partial^2 \Pi_{Strain}}{\partial c_i \partial a_j},\ i = 1.....N,\ \ j = 1.....N, \tag{24}$$

$$H_{ij} = \frac{\partial^2 \Pi_{Strain}}{\partial c_i \partial b_j},\ i = 1.....N,\ \ j = 1.....N, \tag{25}$$

$$K_{ij} = \frac{\partial^2 \Pi_{Strain}}{\partial c_i \partial c_j},\ i = 1.....N,\ \ j = 1.....N. \tag{26}$$

Elements of modal force vector are:

$$F_{1i} = -\frac{\partial \Pi_e}{\partial a_i},\ i = 1.....N, \tag{27}$$

$$F_{2i} = -\frac{\partial \Pi_e}{\partial b_i},\ i = 1.....N, \tag{28}$$

$$F_{3i} = -\frac{\partial \Pi_e}{\partial c_i},\ i = 1.....N. \tag{29}$$

Appendix B

Elements of the residual vector $[R]$ and the tangent matrix $[T]$ are:

$$R_i = \frac{\partial \Pi_{total}}{\partial a_i},\ i = 1, ...N, \tag{30}$$

$$R_i = \frac{\partial \Pi_{total}}{\partial b_i},\ i = N+1, ...2N, \tag{31}$$

$$R_i = \frac{\partial \Pi_{total}}{\partial c_i},\ i = 2N+1, ...3N. \tag{32}$$

$$T_{ij} = \frac{\partial R_i}{\partial a_j},\ i = 1, ...3N,\ j = 1, ...N \tag{33}$$

$$T_{ij} = \frac{\partial R_i}{\partial b_i},\ i = 1, ...3N,\ j = N+1, ...2N \tag{34}$$

$$T_{ij} = \frac{\partial R_i}{\partial c_i},\ i = 1, ...3N,\ j = 2N+1, ...3N \tag{35}$$

Acknowledgements

This work was supported by the Engineering and Physical Sciences Research Council through the EPSRC Centre for Doctoral Training in Advanced Composites for Innovation and Science [grant number EP/G036772/1]. QA would like to acknowledge the China Scholarship Council for partially funding his study at the University of Bristol.

References

1. Vinson J.R. Sandwich structures. *Applied Mechanics Reviews* 2001; **54(3)**:201-214.
2. Yu W, Volovoi V.V, Hodges D.H, Hong X. Validation of the variational asymptotic beam sectional analysis. *AIAA Journal* 2002; **40(10)**:2105-2113.
3. Morandini M, Chierichetti M, Mantegazza P. Characteristic behaviour of prismatic anisotropic beam via generalised eigenvectors. *International Journal of Solids and Structures* 2010; **47**:1327-1337.
4. Rao D.K. Static response of stiff-cored unsymmetric sandwich beams. *Journal of Manufacturing Science and Engineering* 1976; *98(2)*:391-396. DOI:10.1115/1.3438886.

5. Jeon J.S, Hong C.S. Bending of tapered anisotropic sandwich plates with arbitrary edge conditions. *AIAA Journal* 1992; **30(7)**:1762-1769.
6. Frostig Y, Baruch M, Vilnay O, Sheinman I. High-order theory for sandwich beam behaviour with transverse flexible core. *Journal of Engineering Mechanics* 1992; **118**:1026-1043;
7. Frostig Y. Bending of curved sandwich panels with a transversely flexible core-closed-form high-order theory. *Journal of Sandwich Structures and Materials* 1999; **1**4-41.
8. Peled D, Frostig Y. High-order bending of sandwich beams with transversely flexible core and nonparallel skins. *Journal of Engineering Mechanic*1994; **120(6)**:1255-1269.
9. Paydar N, Libove C. Stress analysis of sandwich plates with unidirectional thickness variation. *Journal of Applied Mechanics* 1986; **53(3)**:609-613.
10. Libove C, Lu C.H. Beam-like bending of variable-thickness sandwich plates. *AIAA Journal* 1989; **27(4)**:500-507.
11. Vel S.S, Caccese V, Zhao H. Elastic coupling effects in tapred sandwich panels with laminated anisotropic composite facings.*Journal of Composite Materials* 2005; **39(24)**:2161-2183.
12. Dariushi S., Sadighi M. A new nonlinear high order theory for sandwich beams: an analytical and experimental investigation.*Composite Structures* 2014; **108**:779-788.
13. Paydar N, Libove C. Bending of sandwich plates of variable thickness. *Journal of Applied Mechanics* 1988; **55(2)**:419-424.
14. Zenkour A.M. A comprehensive analysis of functionally graded sandwich plates: Part 1-deflection and stresses. *International Journal of Solids and Structures* 2005; **42**:5224-5242.
15. Zenkour A.M. A comprehensive analysis of functionally graded sandwich plates: Part 2-buckling and free vibration. *International Journal of Solids and Structures* 2005; **42**:5243-5258.
16. Tounsi A, Houari M.S.A, Benyoucef S, Bedia E.A.A. A refined trigonometric shear deformation theory for thermoelastic bending of functionally graded sandwich plates. *Aerospace Science and Technology* 2013; **24**:209-220.
17. Houari M.S.A, Tounsi A, Beg O.A.Thermoelastic bending analysis of functionally graded sandwich plates using a new higher order shear and normal deformation theory. *International Journal of Mechanical Sciences* 2013; **76**:102-111.
18. Kien N.D. Large displacement response of tapered cantilever beams made of axially functionally graded material. *Composites: Part B* 2013; **55**:298-305.
19. Sarkar K, Ganguli R. Closed-form solutions for axially functionally graded Timoshenko beams having uniform cross-section and fixed-fixed boundary condition.*Composites: Part B* 2014; **58**:361-370.

20. Shahba A, Attarnejad R, Marvi M.T, Hajilar S. Free vibration and stability analysis of axially functionally graded tapered Timoshenko beams with classical and non-classical boundary conditions. *Composites: Part B* 2011; **42**:801-808.
21. Huang Y, Li X.F. An analytic approach for exactly determining critical loads of buckling of nonuniform columns. *International Journal of Structural Stability and Dynamics* 2012; **12(4)**: 1250027-1:13.
22. Reddy J.N. *Energy principles and variational methods in applied mechanics* 2002 2nd ed. New York, Wiley.
23. Jones RM. *Mechanics of composite materials* 2nd edn; Taylor and Francis:Philadelphia, 1999; 190-202.
24. Reddy J.N. *An introduction to nonlinear finite element analysis* 2004. Oxford University Press.
25. Pirrera A, Avitabile D, Weaver M.P. Bistable plates for morphing structures: a refined analytical approach with high-order polynomials. *International Journal of Solids and Structures* 2010; **47**:3412-3425.
26. Monterrubio L.E., Iianko S. Proof of convergence for a set of admissible functions for the RayleighRitz analysis of beams and plates and shells of rectangular planform. *Computers and Structures* 2015; **147**:236-243.
27. Kim J, Swanson S.R. Design of sandwich structures for concentrated loading. *Composite Structures* 2001; **52**:365-373.
28. Tessler A., Di Sciuva M.,Gherlone M. *Refined ZigZag theory for laminated composite and sandwich plates.* Technical Pulication -2009-215561, National Aeronautics and Space Administration (2009).
29. Wu Z., Weaver P.M., Raju G., Kim B.C. Buckling analysis and optimisation of variable angle tow composite plates. *Thin-Walled Structures* 2012; **60**:163-172.